Nanoscale

Accepted Manuscript

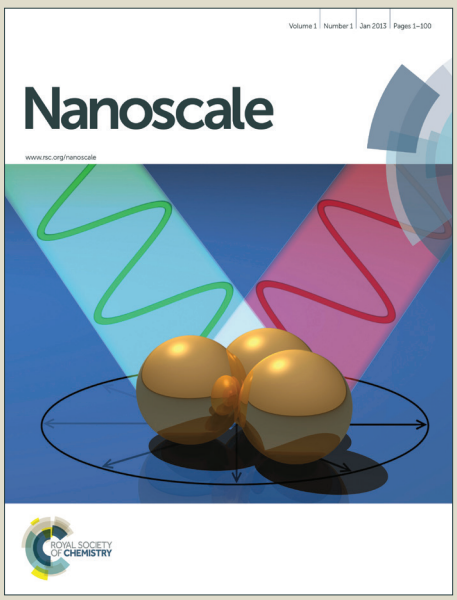

ROYAL SOCIETY OF CHEMISTRY

www.rsc.org/nanoscale

ARTICLE TYPE www. rsc.org/xxxxxx | XXXXXXXX

Molecular resolution friction microscopy of Cu phthalocyanine thin films on dolomite (104) in water

Pawel Nita,[a] Carlos Pimentel,[b,c] Feng Luo,*[a] Begoña Milián-Medina,[a] Johannes Gierschner,[a] Carlos M. Pina,[b,c] and Enrico Gnecco*[a]

Received Xth XXXXXXXXXX 20XX, Accepted Xth XXXXXXXXX 20XX
First published on the web Xth XXXXXXXXXX 200X
DOI: 10.1039/b000000x

The reliability of ultrathin organic layers as active components for molecular electronics depends ultimately on an accurate characterization of the layer morphology and ability to withstand mechanical stresses on the nanoscale. To this end, since the molecular layers need to be electrically decoupled using thick insulating substrates, the use of AFM becomes mandatory. Here, we show how friction force microscopy (FFM) in water allows us to identify the orientation of copper(II)phthalocyanine (CuPc) molecules previously self-assembled on a dolomite (104) mineral surface in ultra-high vacuum. The molecular features observed in the friction images show that the CuPc molecules are stacked in parallel rows with no preferential orientation with respect to the dolomite lattice, while the stacking features resemble well the single CuPc crystal structure. This proves that the substrate induction is low, and makes friction force microscopy in water a suitable alternative to more demanding dynamic AFM techniques in ultra-high vacuum.

1 Introduction

Organic optoelectronic devices have attracted much attention during the last decades. Since the device operation depends critically on a controlled morphology in the active layer, rapid and technically facile methods are required to monitor the controlled growth of molecular structures at a (sub)nanometer scale[1,2]. For device application, the active layers are grown on thick insulating substrates, so that scanning tunneling microscopy (STM) is not a feasible option, and atomic force microscopy (AFM) has to be applied to image the self-assembled molecular structures. However, standard AFM in ambient conditions provides only limited molecular resolution[3]. On the contrary non-contact (NC) AFM under ultra-high vacuum (UHV) conditions has been successfully applied for a number of thin film structures[4–7], but this technique is highly demanding and its applicability is therefore limited. To overcome these problems, we propose a powerful alternative for imaging organic thin films, that is friction force microscopy (FFM) in water using ultrasharp Si_3N_4 probing tips. Exploiting the variations of the lateral force, caused by the periodic interaction between tip and surface, and the negligible adhesion experienced in liquid, benzene rings standing upright are readily identified. We remark that lattice resolution has been actually achieved in recent FFM measurements in ambient conditions (see[8] and[9], where the molecular orientation of self-assembled monolayers could be unambiguously determined in this way). Still, to the best of our knowledge, intramolecular features as those reported here have never been resolved using FFM out of a vacuum so far.

The subject of our investigation are copper(II)phthalocyanine (CuPc) islands, which self-assembled on the (104) surface of a dolomite ($CaMg(CO_3)_2$) crystal of natural origin upon deposition in UHV and were subsequently imaged by FFM in water. CuPc molecules are intensively investigated for device applications due to their thermal and chemical stability and their optical and electronic properties making them attractive compounds in organic (opto)electronics[11,12]. CuPc molecules self-assemble in stacks, which have been extensively studied on metallic surfaces[13–16], graphite[17], semiconductors[18], insulators[19,20], and on top of insulating layers[21], where the orientation of the stacks is significantly influenced by nature[19,21,22] and roughness[19] of the substrate. The dolomite (104) surface has essentially the same crystal structure and similar unit cell dimensions as those of the calcite (104) surface used in the UHV experiments by Hauke et al.[7]. A substantial difference is the ordered replacement of half of Ca cations in calcite by Mg cations in the dolomite structure. Dolomite is much less soluble in water than calcite, which allowed us to perform reproducible measurements on a time scale of few days.

[a] *Instituto Madrileño de Estudios Avanzados en Nanociencia (IMDEA Nanociencia), Ciudad Universitaria de Cantoblanco, E-28049, Madrid, Spain.*
[b] *Departamento de Cristalografía y Mineralogía, Universidad Complutense de Madrid, E-28040 Madrid, Spain.*
[c] *Instituto de Geociencias IGEO, UCM-CSIC, c/ José Antonio Novais 2, E-28040 Madrid, Spain.*

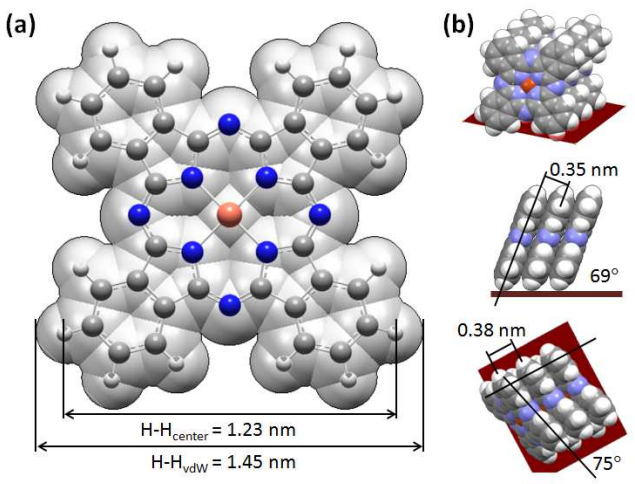

Fig. 1 (a) Chemical structure of a copper(II) phthalocyanine (CuPc) molecule as resulting from DFT calculations; the corresponding van der Waals (vdW) overlapping sphere model is shown in the background. (b) Molecular stack geometry as determined from single crystal x-ray diffraction[10]. Intra-stack periodicity (0.38 nm), π-π stacking distance (0.35 nm), and inclinations of the molecular planes against the stacking direction are indicated.

2 Experimental

A dolomite ($CaMg(CO_3)_2$) sample of optical quality from Eugui (Spain) was used as a substrate to deposit the organic molecules. The dolomite (104) surface was prepared in ambient by cleavage of a bulk crystal with a razor blade. The sample was immediately transferred into a UHV chamber with a base pressure around 2×10^{-10} mbar and degassed at 570 K for 1.5 hours in order to remove contaminants and surface charges. CuPc powder with a purity of 99.99% was purchased from Sigma-Aldrich Inc. After degassing at 570 K for 24 h in a Organics KENTAX Triple Evaporator, CuPc was sublimed in situ on the dolomite (104) surface at room temperature. The source temperature was 625 K and the chamber pressure was less than 2×10^{-9} mbar during deposition. A growth rate of 0.1 monolayer/min was determined by quartz balance. The sample so prepared was immersed in liquid a few minutes after taking it out of the UHV chamber. The AFM measurements were performed in a liquid cell filled with deionised water (Milli-Q Millipore with specific resistivity 18 MΩ cm) at room temperature (RT). A commercial AFM system Cervantes (Nanotec, Tres Cantos, Spain) was used, with silicon cantilevers holding integrated ultrasharp tips (Bruker SNL-10). These sensors have typical resonance frequencies of 80-180 kHz, a spring constant of 0.01-0.05 N/m, and nominal tip radius of 2 nm. The normal and lateral forces were calibrated using the method by Noy et al.[23]. Molecular res-

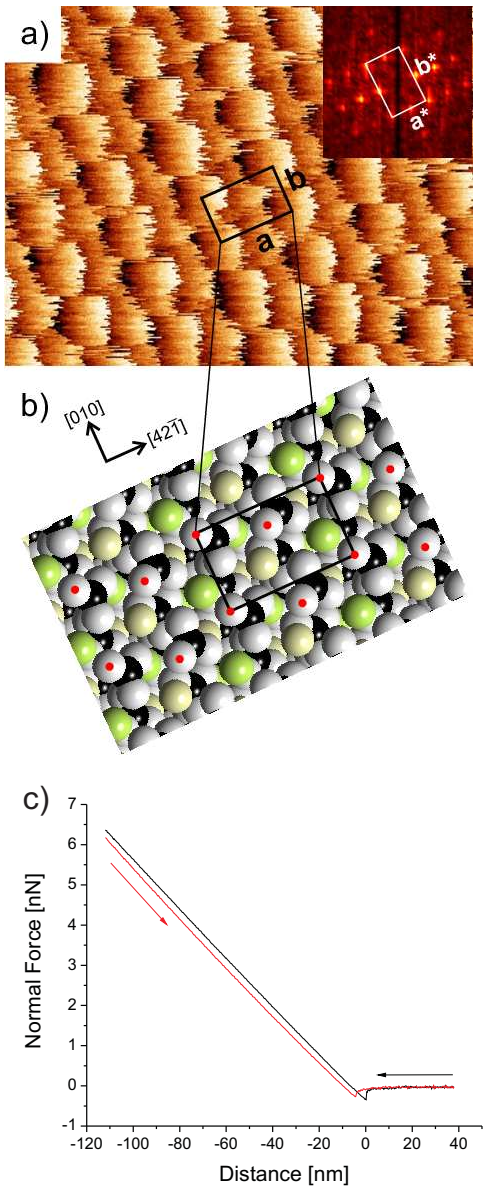

Fig. 2 (a) High resolution FFM image (4.8×3.3 nm^2) and corresponding Fast Fourier Transform map (inset) of dolomite (104) surface. Measurements have been performed in water, with a scan rate of 16 Hz and a normal force $F_N = 4.6$ nN, corresponding to an average friction force $F_L = 9.9$ nN. (b) Structural model of dolomite (104) surface (top view) with marked unit cell. Oxygen atoms are represented by white spheres, C atoms by black spheres, Ca atoms are yellow and Mg atoms are green. Protruding O atoms are highlighted by red dots. (c) Force-distance curve when the AFM is approached (black curve) and retracted (red curve) on dolomite (104) in water. Note the low value (≈ 0.3 nN) of the pull-off force.

olution could be achieved at high scanning rate (16 Hz with 512 points per line). The AFM images were processed using WSxM software[24]. The geometry of CuPc was calculated by density functional theory (DFT) employing the B3LYP functional under the spin-unrestricted formalism and the 6-311G* basis set as defined in the Gaussian09 program package[25].

3 Results and discussion

CuPc is a neutral metal-centered planar molecule with four-fold symmetry (point group D_{4h}), see Fig. 1(a). CuPc shows a strong aggregation tendency, forming stacked arrangements driven by enthalpic (dense packing) arguments as well as by π-π interaction. In the single crystal[10] (one molecule per unit cell; space group $P\bar{1}$) it forms stacked structures with an interplane distance of 0.35 nm, while the Cu-Cu distances (i.e. the intra-stack periodicity) are 0.38 nm, see Fig. 1(b). This is due to an inclination of the CuPc plane against the stacking direction of 69° and a lateral displacement along the stack corresponding to an inclination of 75° with respect to the molecular plane. Upon deposition onto substrates from solution or in vacuum, the orientation of the CuPc stacks are significantly influenced by structure[19,21,22] and roughness[19] of the substrate, resulting in flat-lying or standing molecules with respect to the substrate.

In Fig. 2(a) a high resolution FFM image of the dolomite (104) surface in water, prior to molecular deposition, is shown. Atomic rows running along the [010] and [42$\bar{1}$] directions are clearly seen. The rectangular unit cell of the surface crystal is highlighted. The values of the lattice constants, as estimated from this image, are $a = 0.81$ nm in the [42$\bar{1}$] direction and $b = 0.51$ nm in the [010] direction. These values are consistent with recent AFM measurements performed with a different setup[26,27]. The zigzag alignment of the spots suggests that the the contrast is due to the interaction of the tip apex with the O atoms protruding out of the surface rather than with the Mg^{2+} or the Ca^{2+} cations in the unit cell, which, as shown in Fig. 2(b), are aligned in straight lines.

Fig. 3 shows a topographic image of dolomite covered by about 2.0 monolayers of CuPc. Elongated molecular islands with height of about 4.5 nm are seen all over the surface. The width of these structures varies between 200 and 600 nm, and their length is in the order of 1-3 μm. The strips do not reveal any preferential orientation, suggesting that the intermolecular interactions are much stronger than the interaction between molecules and substrate. This can be seen in Fig. 4, where the angular distribution of 30 molecular strips on a 12×12 μm^2 area is compared to the length and width distribution of the same strips.

To investigate the internal structure of the molecular islands, we attempted to perform high resolution scanning over several of them. This was not possible in standard topographic images, whereas FFM images showed sub-molecular features, like those shown in Fig. 5. Here, the average lateral force between tip and molecules was $F_L = 5.5$ nN. The friction image allows us to recognize a stacked intermolecular arrangement. The molecular stacks run along the axis of the corresponding strip and, consequently, they do not show any preferential orientation with respect to the substrate. Two elongated spots per molecule are unambiguously identified. Intermolecular structural parameters can be estimated from the 2D self-correlation analysis shown in the inset, which was performed along and perpendicular to the stacking direction. Along the stack, the periodicity is 0.36 nm, very similar to the reported periodicity from the single crystal x-ray value (0.38 nm). The measured stack width is 1.3 nm, while the vdW stack width calculated from single crystal data is 1.45 nm $\times \sin 75^\circ$ = 1.40 nm. This indicates an interdigitated structure of neighboring CuPc stacks on dolomite just like in the single crystal which should effectively reduce the stack width by roughly the vdW radius of hydrogen (0.11 nm), resulting in a value of 1.29 nm, in perfect agreement with the measured value. Accordingly, the crystal structure stack (projected against the stacking plane)

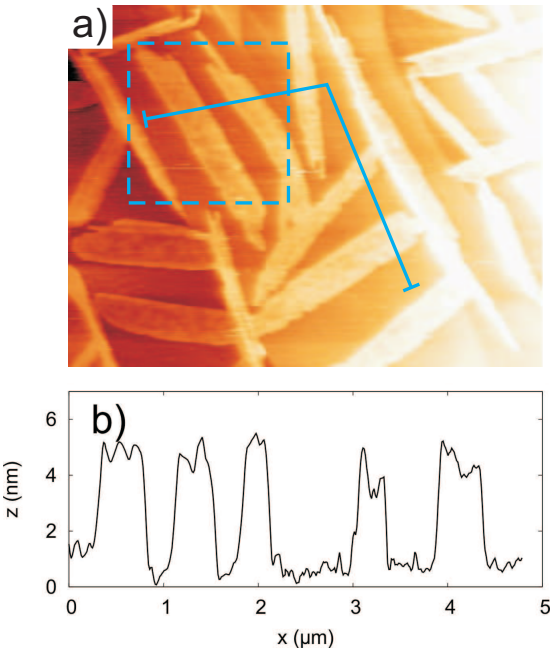

Fig. 3 (a) Contact mode AFM topography (4.6×6 μm^2) of the dolomite (104) surface covered by 2.0 monolayers of CuPc. Imaging was performed in deionized water at room temperature with a normal force $F_N = 2.7$ nN. CuPc molecules, due to high mobility and intermolecular interactions formed elongated islands without any preferential orientation with respect to the substrate. The square region (1.8×1.8 μm) limited by the dashed lines will be repeatedly scanned (and damaged) in Fig. 6. (b) Topography profile taken along the continuous line in (a).

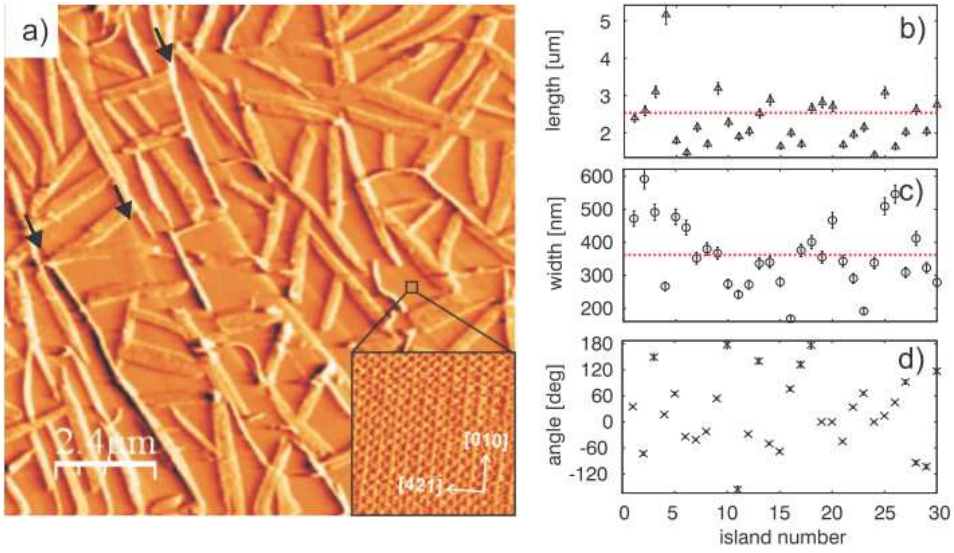

Fig. 4 (a) AFM error signal ($12\times12\ \mu m^2$) of a different region of the dolomite (104) surface covered by CuPc. The inset shows the dolomite lattice in a region which has not been covered by the molecules. (b) Length distribution, (c) width distribution and (d) angular distribution of 30 molecular strips selected from (a). The dotted lines represent the average length and width values respectively.

can be perfectly overlaid with the FFM image, see Fig. 5. In this way, we can conclude that the friction spots correspond to standing benzene rings. The good agreement of the stacking structure on dolomite with the single crystal data gives full evidence that substrate induction is weak on dolomite, and the growth of CuPc is essentially driven by self-assembly.

The contrast in the FFM map in Fig. 5, not achieavable in standard topography, is caused by the lateral motion of the probing tip. In this context the benzene rings of the CuPc molecules act as pinning centers for the tip apex. When the lateral force reaches a critical value, pinning becomes unsustainable and the tip slips towards an adjacent ring in the same molecule or in a neighbor one. Note that the slip process does not occur as fast as on dolomite (Fig. 2a), where the borders of the pinning sites (corresponding to the protruding O atoms) appear sharper. This is possibly due to a larger number of atoms forming the contact area, as observed by Maier *et al.*[28] in their numeric simulations of slip duration with a different number of bonding sites at the tip apex. In this context, we remark that no isolated molecules nor defects nor step edges could be imaged in our measurements, which prevents us from claiming that true sub-molecular resolution was achieved. Nevertheless, subnanometric contrast variations observed in the friction images can be clearly attributed to the orientation of benzene rings in the stacking pattern of CuPc molecules depicted in Fig. 1, allowing us to reconstruct the molecular arrangement with respect to the substrate.

Regarding the improved resolution achieved in water, which is the key point of this paper, we note that a recent study based on frequency modulation AFM visualized the ordered adsorption of water molecules on a hydrophilic mica surface[29]. Whether the AFM tip interacts mainly with the adsorbed water molecules or with the substrate lattice is a current theme of debate. However, the influence of the hydration layer becomes questionable in our case, since we have achieved molecular resolution on both the hydrophilic dolomite substrate and the (slightly) hydrophobic CuPc adsorbate using the same probing tip. Thus, other mechanisms than short range chemical forces must play a key role. The most important of them is the removal of capillary forces in water. This effect leads to a strong reduction of adhesion between tip and surface, as attested by Fig. 2(c). Ultimately, it may result into less damage of the dolomite substrate and, especially, of the molecular film when the tip is being scanned.

On the dolomite surface strong local variations in surface charge are induced by the alternate arrangement of Ca, Mg and carbonate (Fig. 2b). As a result, water molecules can easily adsorb onto the surface with the oxygen facing Ca or Mg and the hydrogen atoms oriented towards the carbonates[30,31]. On the other side, the composition of the tip apex is essentially unknown. The tip may be terminated by silica cluster with significantly charged cations, or, since the tip is in contact with the sample all time, it can be also covered with small clusters picked up from the dolomite surface. In both cases, we expect that the water molecules will adsorb quite strongly onto the tip. Nevertheless, these effects are present also when imaging

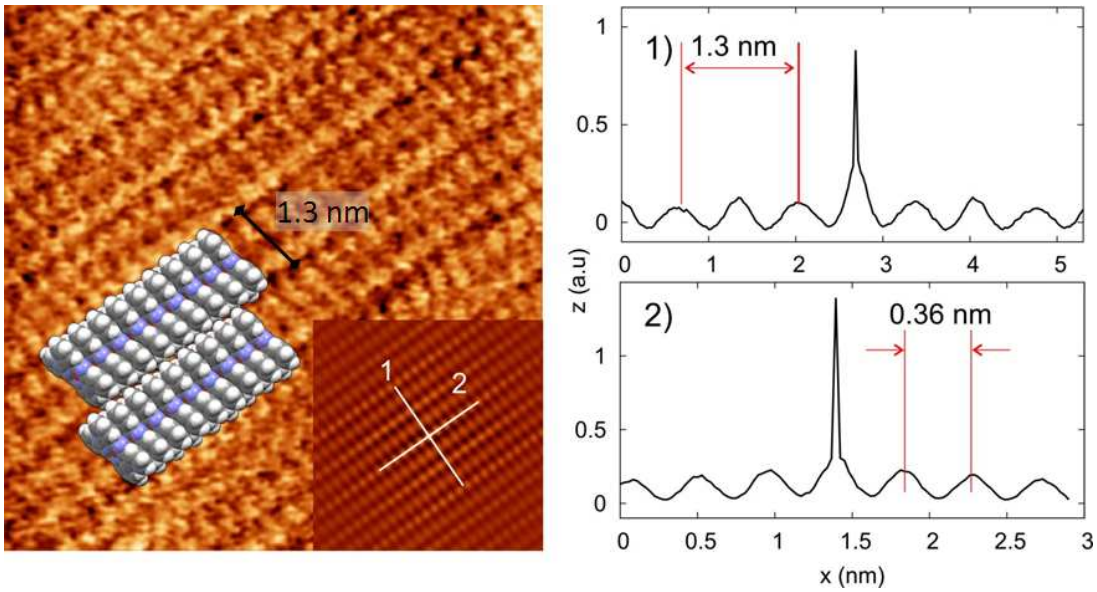

Fig. 5 High resolution friction map (10×10 nm^2) on a CuPc island. The periodic arrangement of the molecules in parallel stacks, running along the axis of the island, is clearly visible. The average friction force is 5.5 nN (corresponding to a normal force $F_N = 2.7$ nN). Inset shows a 2D self-correlation of the friction map. Two profiles corresponding to the white lines 1 and 2 are shown on the right side.

in ambient conditions, where a water layer always covers the sample surface. For this reason, we believe that the charge state of tip and surface, even if it determines the nature of the local interaction forces involved in the imaging process, cannot explain the better resolution achieved in water. Again, the most reasonable explanation for it is the lack of capillary effects in this environment.

When the normal force F_N increases, so do the pinning effect and the lateral force, and the resolution achieved via the stick-slip mechanism is enhanced. Nevertheless, this can also lead to irreversible damage of the molecular film. The images presented in Figures 3 and 5 correspond to a threshold value of the normal force $F_N = 2.7$ nN. If the same area is repeatedly scanned while keeping this value, the molecular layers are gradually worn off. This is seen in Fig. 6, where three 'snapshots' of the abrasive process at different times are shown. Two layers are progressively removed till the step edges of the underlying dolomite (104) surface become clearly visible in Fig. 6(c). Note that, before being worn off, the molecular strips were running across the step edges of the substrate in a carpet-like fashion. This gives another indication of the weak interaction between CuPc and the dolomite surface.

4 Conclusions

In summary, we have presented a powerful method for imaging with molecular resolution of semiconducting organic films, that is FFM in water using ultrasharp Si_3N_4 probing tips. The potential of this technique was demonstrated on CuPc stacks on an insulating dolomite surface, revealing details of the molecular stacking features. The CuPc molecules are found to form elongated islands a few microns long which are randomly oriented with respect to the substrate lattice. Within each island, the molecules are stacked in parallel rows, where the stacking and inter-stacking architecture essentially resemble the single crystal structure, i.e. driven by π-π stacking and dense packing constraints. Noticeably, no molecules could be observed in similar measurements performed in ambient conditions. Thus, due to possible detrimental impact of water to device functioning, the method proposed here cannot be used as an *in situ* method for organic optoelectronic devices. However, it will be an excellent fast, cheap and powerful morphological and mechanical characterization method of organic-mineral structures compared with other *ex situ* scanning probe techniques (performed under ultra-high vacuum and low temperature conditions). Importantly, friction force microscopy in water can be extended to characterize other molecular films and even thick single crystals, with important applications in the development of new organic optoelectronic devices.

5 Acknowledgments

This work was supported by the Spanish Ministerio de Economía y Competitividad (MINECO; project MAT2012-34487). C.P is grateful to Spanish Ministry of Education, Cul-

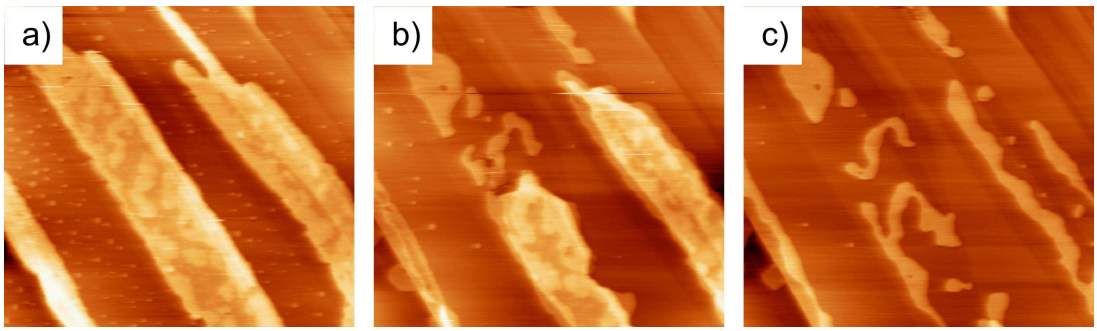

Fig. 6 Effect of prolonged scanning on the square region highlighted in Fig. 3. The topographic images (a), (b) and (c) were acquired while scanning that region back and forth for the 3rd, 19th and 22nd time respectively. Note the progressive damage of the molecular strips and the appearance of the substrate step edges previously buried by the CuPc molecules.

ture and Sports for a FPU grant.

References

1 M. Böhringer, K. Morgenstern, W.-D. Schneider, R. Berndt, F. Mauri, A. D. Vita and R. Car, *Phys. Rev. Lett.*, 1999, **83**, 324–327.
2 G. Pawin, K. L. Wong, K.-Y. Kwon and L. Bartels, *Science*, 2006, **313**, 961–962.
3 E. Meyer, L. Howald, R. Overney, H. Heinzelmann, H.-J. Güntherodt, T. Wagner, H. Schier and S. Roth, *Nature*, 1991, **349**, 398–400.
4 L. Nony, E. Gnecco, A. Baratoff, A. Alkauskas, R. Bennewitz, O. Pfeiffer, S. Maier, A. Wetzel, E. Meyer and C. Gerber, *Nano Lett.*, 2004, **4**, 2185–2189.
5 J. M. Mativetsky, S. A. Burke, S. Fostner and P. Grutter, *Nanotechnology*, 2007, **18**, 105303.
6 S. Maier, L.-A. Fendt, L. Zimmerli, T. Glatzel, O. Pfeiffer, F. Diederich and E. Meyer, *Small*, 2008, **4**, 1115–1118.
7 C. M. Hauke, P. Rahe, M. Nimmrich, J. Schütte, M. Kittelmann, I. G. Stará, I. Starý, J. Rybáček and A. Kühnle, *J. Phys. Chem. C*, 2012, **116**, 4637–4641.
8 J. Chen, I. Ratera, A. Murphy, D. F. Ogletree, J. M. J. Fréchet and M. Salmeron, *Surf. Sci.*, 2006, **600**, 4012.
9 Y. Qi, X. Liu, B. L. M. Hendriksen, V. Navarro, J. Y. Park, I. Ratera, J. M. Klopp, C. Edder, F. J. Himpsel, J. M. J. Fréchet, E. E. Haller and M. Salmeron, *Langmuir*, 2010, **26**, 16522.
10 A. Hoshino, Y. Takenaka and H. Miyaji, *Acta Crystallographica Section B*, 2003, **59**, 393–403.
11 X. Zhou, M. Pfeiffer, J. Blochwitz, A. Werner, A. Nollau, T. Fritz and K. Leo, *Appl. Phys. Lett.*, 2001, **78**, 410–412.
12 J. Blochwitz, M. Pfeiffer, T. Fritz and K. Leo, *Appl. Phys. Lett.*, 1998, **73**, 729–731.
13 K. Manandhar, T. Ellis, K. Park, T. Cai, Z. Song and J. Hrbek, *Surf. Sci.*, 2007, **601**, 3623 – 3631.
14 H. Huang, W. Chen, S. Chen, D. C. Qi, X. Y. Gao and A. T. S. Wee, *Appl. Phys. Lett.*, 2009, **94**, 163304–163307.
15 K. W. Hipps, X. Lu, X. D. Wang and U. Mazur, *J. Phys. Chem.*, 1996, **100**, 11207–11210.
16 M. Stöhr, T. Wagner, M. Gabriel, B. Weyers and R. Möller, *Adv. Fun. Mat.*, 2001, **11**, 175–178.
17 C. Ludwig, R. Strohmaier, J. Petersen, B. Gompf and W. Eisenmenger, *J. Vac. Sci. Technol. B*, 1994, **12**, 1963–1966.
18 A. Tekiel, M. Goryl and M. Szymonski, *Nanotechnology*, 2007, **18**, 475707.
19 M. Nakamura, T. Matsunobe and H. Tokumoto, *J. Vac. Sci. Technol. B*, 1996, **14**, 1109–1113.
20 S. Godlewski, A. Tekiel, J. S. Prauzner-Bechcicki, J. Budzioch and M. Szymonski, *Chem. Phys. Chem.*, 2010, **11**, 1863–1866.
21 R. R. Lunt, J. B. Benziger and S. R. Forrest, *Adv. Mater.*, 2007, **19**, 4229–4233.
22 K. S. Yook, B. D. Chin, J. Y. Lee, B. E. Lassiter and S. R. Forrest, *Appl. Phys. Lett.*, 2011, **99**, 043308–043311.
23 A. Noy, D. C. Frisbie, L. F. Rozsnyai, M. S. Wrighton and C. M. Lieber, *J. Am. Chem. Soc.*, 1995, **117**, 7943–7951.
24 I. Horcas, R. Fernández, J. M. Gómez-Rodríguez, J. Colchero, J. Gómez-Herrero and A. M. Baro, *Rev. of Sci. Instr.*, 2007, **78**, 013705–013713.
25 M. J. Frisch, G. W. Trucks, H. B. Schlegel, G. E. Scuseria, M. A. Robb, J. R. Cheeseman, G. Scalmani, V. Barone, B. Mennucci, G. A. Petersson, H. Nakatsuji, M. Caricato, X. Li, H. P. Hratchian, A. F. Izmaylov, J. Bloino, G. Zheng, J. L. Sonnenberg, M. Hada, M. Ehara, K. Toyota, R. Fukuda, J. Hasegawa, M. Ishida, T. Nakajima, Y. Honda, O. Kitao, H. Nakai, T. Vreven, M. J. A., J. E. Peralta, F. Ogliaro, M. Bearpark, J. J. Heyd, E. Brothers, K. N. Kudin, V. N. Staroverov, R. Kobayashi, J. Normand, K. Raghavachari, A. Rendell, J. C. Burant, S. S. Iyengar, J. Tomasi, M. Cossi, N. Rega, J. M. Millam, M. Klene, J. E. Knox, J. B. Cross, V. Bakken, C. Adamo, J. Jaramillo, R. Gomperts, R. E. Stratmann, O. Yazyev, A. J. Austin, R. Cammi, C. Pomelli, J. W. Ochterski, R. L. Martin, K. Morokuma, V. G. Zakrzewski, G. A. Voth, P. Salvador, J. J. Dannenberg, S. Dapprich, A. D. Daniels, . Farkas, J. B. Foresman, J. V. Ortiz, J. Cioslowski and D. J. Fox, *Gaussian 09 Revision A.1*, Gaussian Inc. Wallingford CT 2009.
26 C. M. Pina, C. Pimentel and M. Garcia-Merina, *Surf. Sci.*, 2010, **604**, 1877–1881.
27 C. M. Pina, R. Miranda and E. Gnecco, *Phys. Rev. B*, 2012, **85**, 073402–073406.
28 S. Maier, Y. Sang, T. Filleter, M. Grant, R. Bennewitz, E. Gnecco and E. Meyer, *Phys. Rev. B*, 2005, **72**, 245418.
29 T. Fukuma, Y. Ueda, S. Yoshioka and H. Asawaka, *Phys. Rev. Lett.*, 2010, **104**, 016101.
30 S. Stipp, *Geochim. Cosmochim. Acta*, 1999, **63**, 3121.
31 E. Escamilla-Roa, C. Sainz-Diaz, F. Huertas and A. Hernandez-Laguna, *Journ. Phys. Chem. C*, 2013, **117**, 17583.